

Supporting Information for

Destabilization of Marine Gas Hydrate-Bearing Sediments induced by a Hot Wellbore: A Numerical Approach

Authors: Tae-Hyuk Kwon ¹, Ki-Il Song ², and Gye-Chun Cho ^{3*}

Affiliations:

¹ Postdoctoral Research Fellow, Earth Sciences Division,
Lawrence Berkeley National Laboratory, 1 Cyclotron Rd. Berkeley, CA 94720, U.S.A.
Email: thkwon@lbl.gov

² Associate Professor, Faculty of Civil Engineering,
University Technology MARA Malaysia, 40450 Shah Alam, Selangor, Malaysia
Email: kiilsong@kaist.ac.kr

^{3*} Corresponding Author
Associate Professor, Department of Civil and Environmental Engineering,
Korea Advanced Institute of Science and Technology (KAIST), Daejeon 305-701, Korea
Email: gyechun@kaist.edu

Contents

		Page
Appendix S1	Analytical formulations for hydrate dissociation in sediments	S2
Figure S1	Spatial distribution of the free gas saturation for the case REF.	S5
Figure S2	Spatial distribution of the effective stress for the case REF	S7
Figure S3	Deformation features of the formation for the case REF.	S9

*Corresponding author phone: (+82) 42-350-3622; email: gyechun@kaist.edu

APPENDIX S1. ANALYTICAL FORMULATIONS FOR HYDRATE DISSOCIATION IN SEDIMENTS

This study uses an analytical model proposed by Kwon et al.⁹ to calculate the excess pore fluid pressure and the volume fraction of methane hydrate during the hydrate dissociation. In the analytical model, when the increase in temperature induces the dissociation, the released fluids raise the pore fluid pressure to the phase equilibrium pressure corresponding to a given temperature. At the same time, the volume fraction of methane hydrate in a unit volume of sediments is calculated during the dissociation, so that the extent of the self-preservation behavior can be determined. The excess pore fluid pressure generated by the hydrate dissociation is related to the amount of methane hydrate consumed. The details of our hydrate dissociation model are as follows (all the notations are listed in Table 1).

Assumptions. The model requires several assumptions: as gas hydrates occur at shallow sediments (less than 1000 mbsf), the changes in densities of phases (i.e., mineral, water, and hydrate) induced by temperature increase is disregarded;⁹ no mass flux occurs during the hydrate dissociation and hydrate dissociation takes place under an equilibrium condition; the kinetic effect on the hydrate dissociation is insignificant—this assumption is valid in the geologic scale because kinetic effects are insignificant for long-term processes (e.g., more than tens of days);⁴⁴ and the capillary effect on the phase equilibrium boundary is not considered.

Generic formulation. The mass of dissociated gas hydrate is derived from the two governing relationships: the mass conservation relationship and the volume change relationship. In accordance with the zero mass flux assumption, the mass of each species is conserved within the boundary during the thermal stimulation of the hydrate-bearing sediments. In particular, the total

mass of the hydrate-forming gas (HFG) remains constant:

$$\begin{aligned} n^{HFG} &= n_{h0}^{HFG} + n_{aq0}^{HFG} + n_{g0}^{HFG} && \text{initial} \\ &= n_h^{HFG} + n_{aq}^{HFG} + n_g^{HFG} && \text{after some dissociation} \end{aligned} \quad (A-1)$$

The total volumetric expansion of the hydrate-bearing sediment is the sum of the volume change experienced by each constituent and equal to the volume expansion of the granular skeleton against the surrounding medium; it is also associated with the increase in pore fluid pressure. As the effective stress is expressed as $\sigma' = \sigma_{tot} - P$, the change in effective stress for a constant overburden stress is $-\Delta\sigma' = \Delta P$; then the volumetric strain is

$$\begin{aligned} \varepsilon &= \frac{-\Delta\sigma'}{B_{sk}} = \frac{\Delta V_t}{V_{t0}} \\ &= \frac{\Delta P}{B_{sk}} = \frac{\Delta V_m}{V_{t0}} + \frac{\Delta V_h}{V_{t0}} + \frac{\Delta V_w}{V_{t0}} + \frac{\Delta V_g}{V_{t0}} \end{aligned} \quad (A-2)$$

The gas hydrate partially dissociates during heating, contributing water to the water phase and gas to the gas phase. The general relation of the pore pressure increase ΔP and the mass of gas hydrate dissociated ΔM_h (which is negative during dissociation) can be obtained as follows (for the details in derivation, refer to Kwon et al.):⁹

$$\varepsilon = \frac{\Delta P}{B_{sk}} = \frac{\Delta M_h}{V_{t0}} \left[\frac{1}{\rho_h} - \frac{1 - R_m}{\rho_w} \right] + \frac{\Delta V_g}{V_{t0}} \quad (A-3)$$

The last term $\Delta V_g / V_{t0}$, which is the volume change of gas normalized by the initial volume of the hydrate-bearing sediment, can be expressed as follows:

$$\frac{\Delta V_g}{V_{t0}} = \frac{n_g^{HFG} RT}{P V_{t0}} - \phi \cdot S_{g0} . \quad (\text{A-4})$$

As long as some hydrate remains in the system, the pressure P for a given temperature T is the corresponding equilibrium pressure P_{eq}^T on the phase boundary. The increase in pressure ΔP when all the hydrate in the system is consumed can be evaluated by using Equations A-3 and A-4 for $\Delta M_h = -M_{h0}$.

Remaining gas hydrate volumetric fraction. Of particular interest is the hydrate mass change ΔM_h during the dissociation (the BC path in Figure 1). This value can be computed by using Equations A-3 and A-4 for a given PT state on the phase boundary (P_{eq}^T, T). The remaining gas hydrate volume fraction S_h is related to ΔM_h through the mass density, and can be expressed as follows with proper consideration of the volumetric strains:

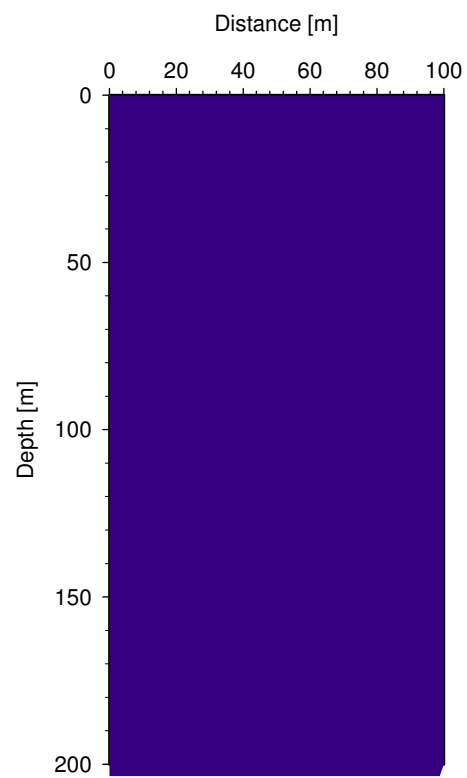
$$S_h = \frac{\phi \cdot S_{h0} + \frac{\Delta M_h}{\rho_h V_{t0}}}{\left(1 + \frac{\Delta P}{B_{sk}}\right) - (1 - \phi)} . \quad (\text{A-5})$$

▪ Additional Reference

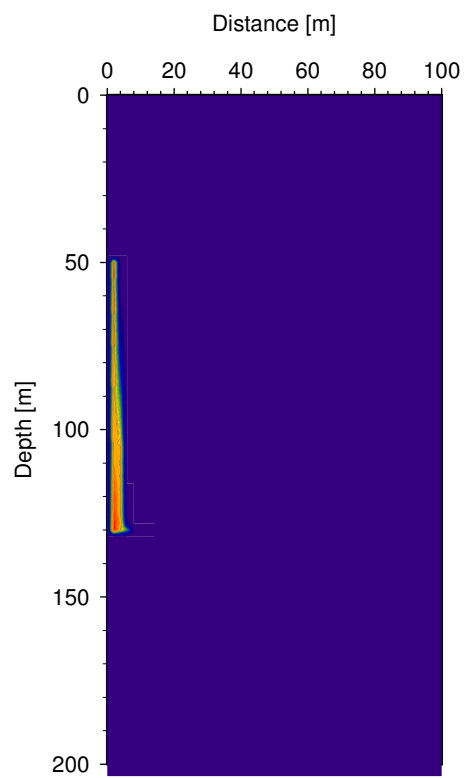
9. Kwon, T. H.; Cho, G. C.; Santamarina, J. C. Gas hydrate dissociation in sediments: Pressure-temperature evolution. *Geochemistry Geophysics Geosystems* **2008**, 9, Q03019, doi:10.10292007GC001920.

44. Kowalsky, M. B.; Moridis, G. J. Comparison of kinetic and equilibrium reaction models in simulating gas hydrate behavior in porous media. *Energy Conversion and Management* **2007**, 48, (6), 1850-1863.

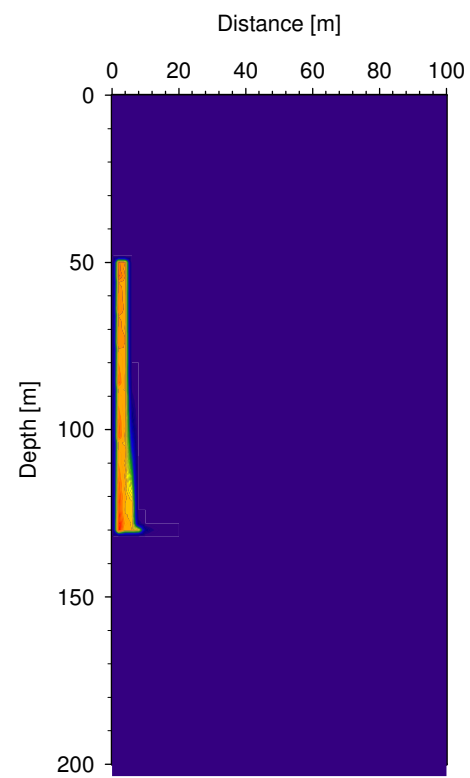
Supporting Figure S1



(a)



(b)



(c)

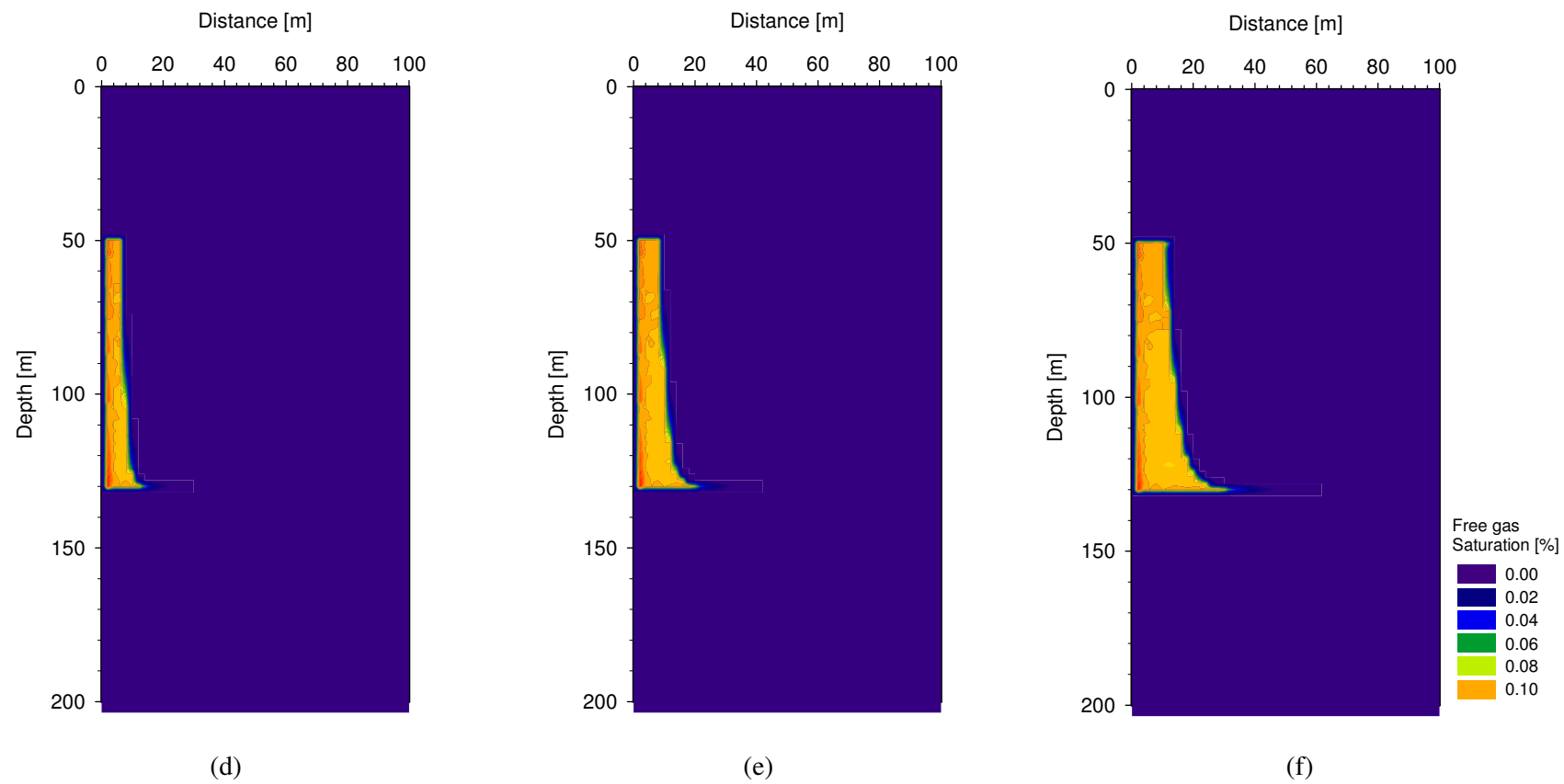
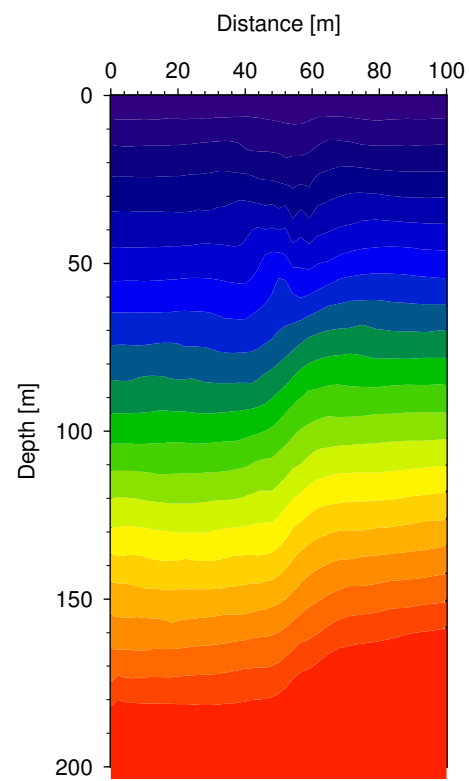
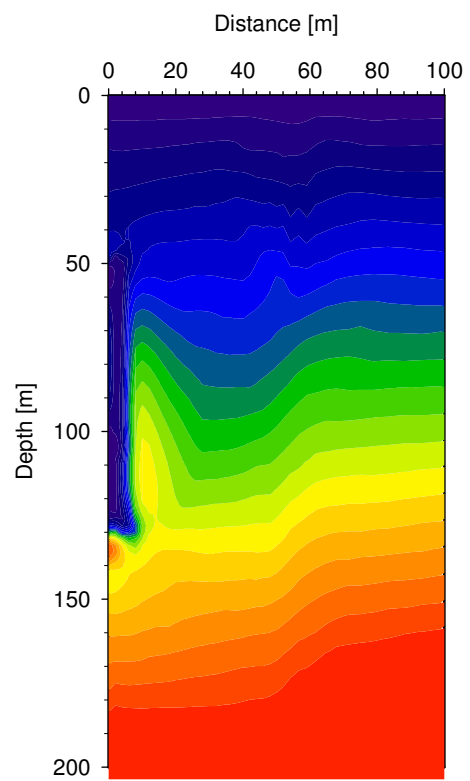


Figure S1. Spatial distribution of the free gas saturation for the case REF: (a) at the initial, (b) after 1 year, (c) after 2 years, (d) after 5 years, (e) after 10 years, and (f) after 20 years.

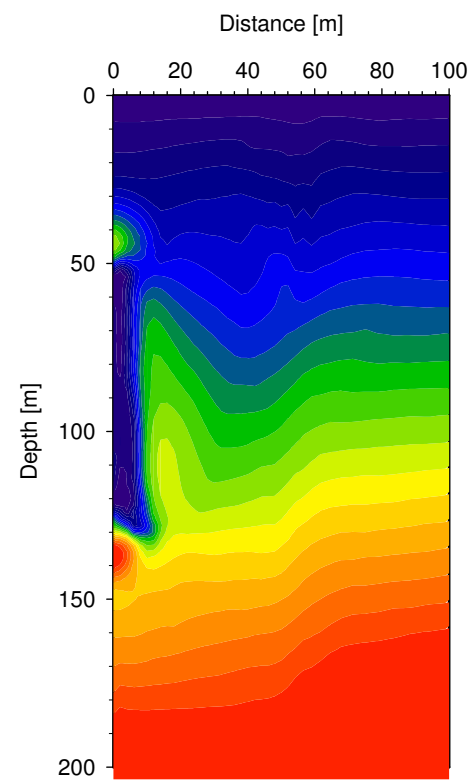
Supporting Figure S2



(a)



(b)



(c)

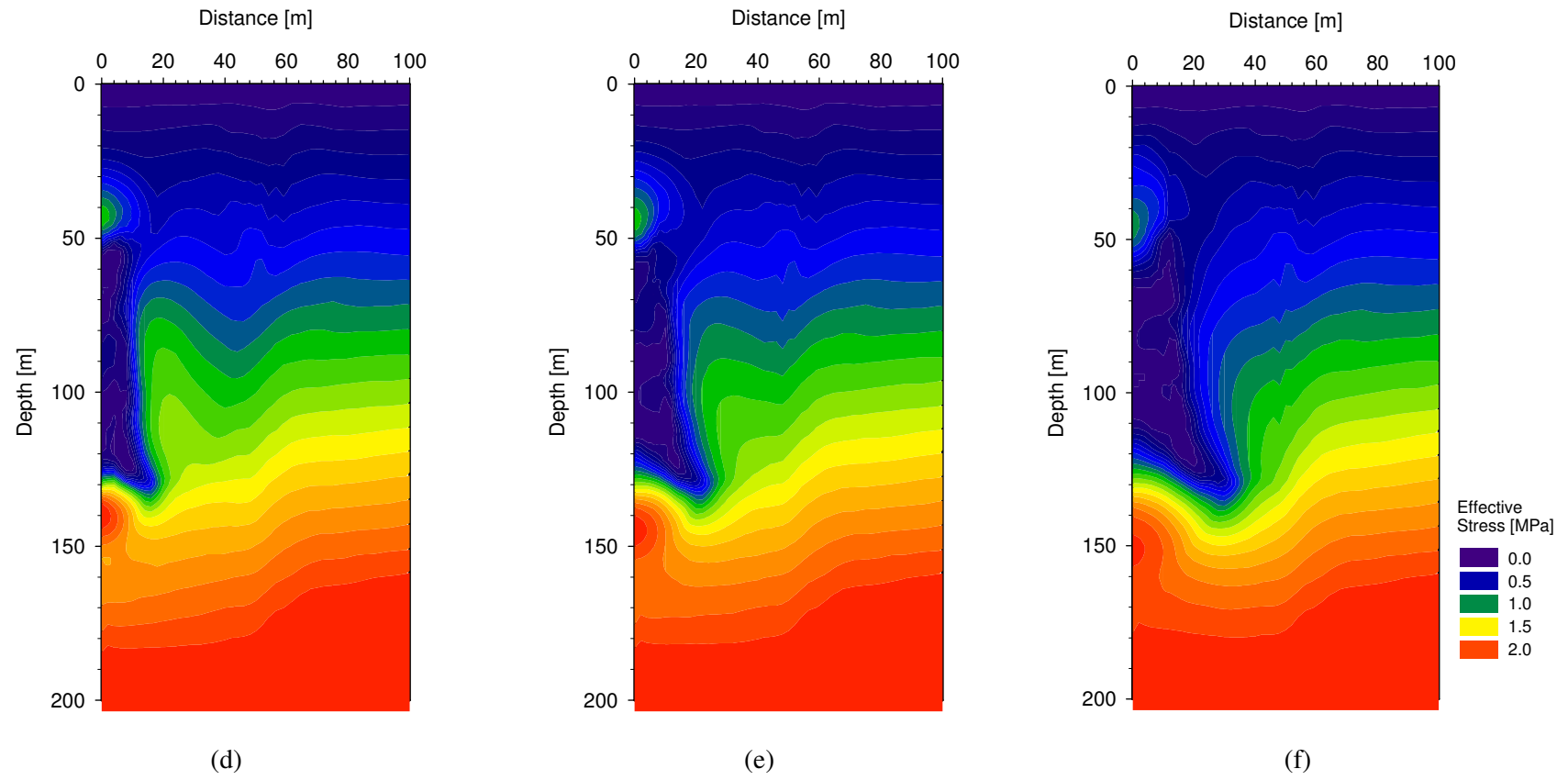
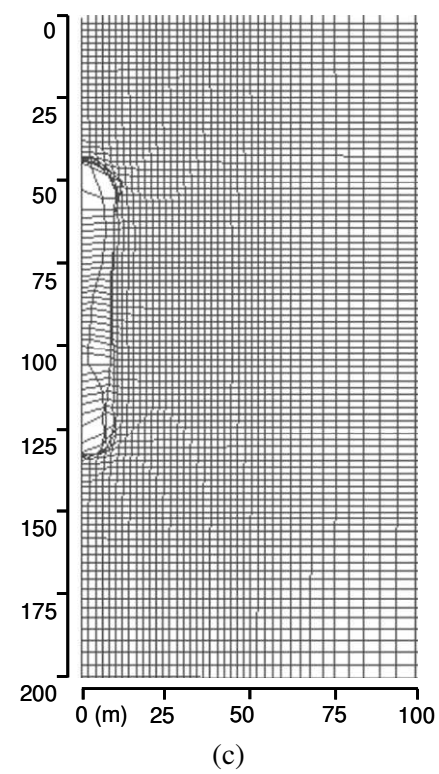
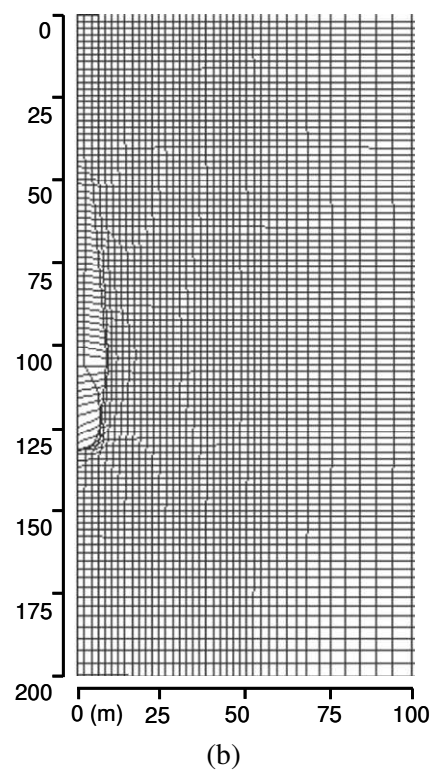
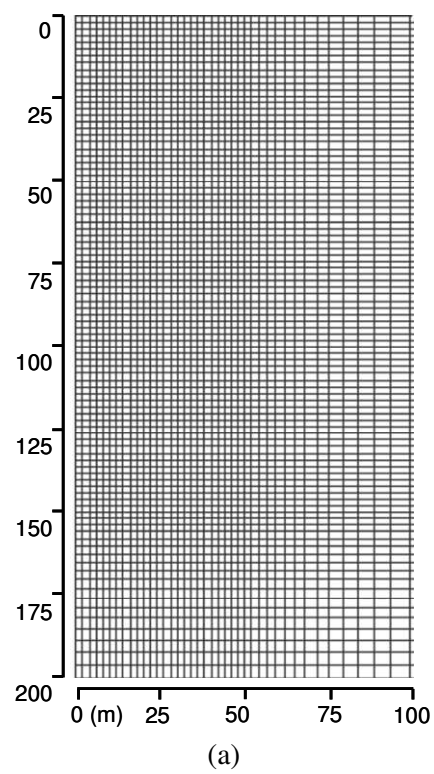


Figure S2. Spatial distribution of the effective stress for the case REF: (a) at the initial, (b) after 1 year, (c) after 2 years, (d) after 5 years, (e) after 10 years, and (f) after 20 years.

Supporting Figure S3



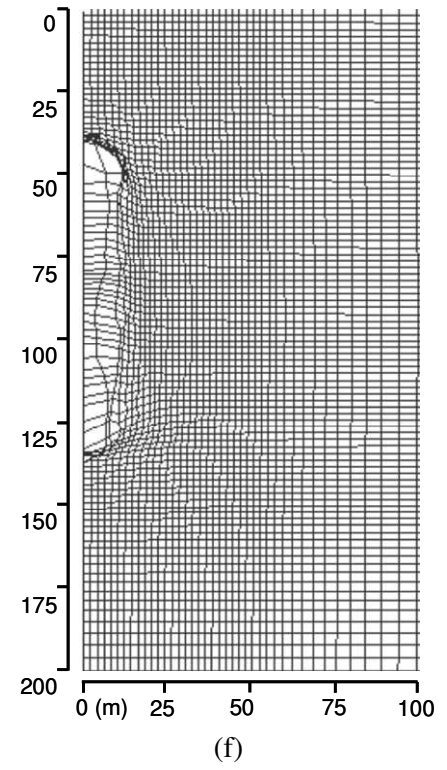
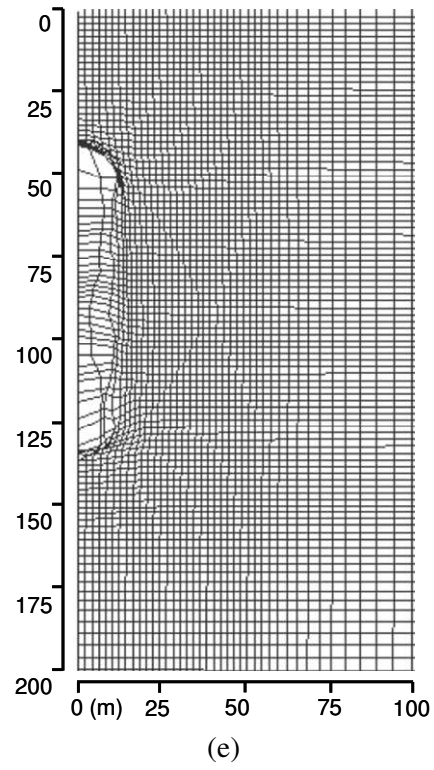
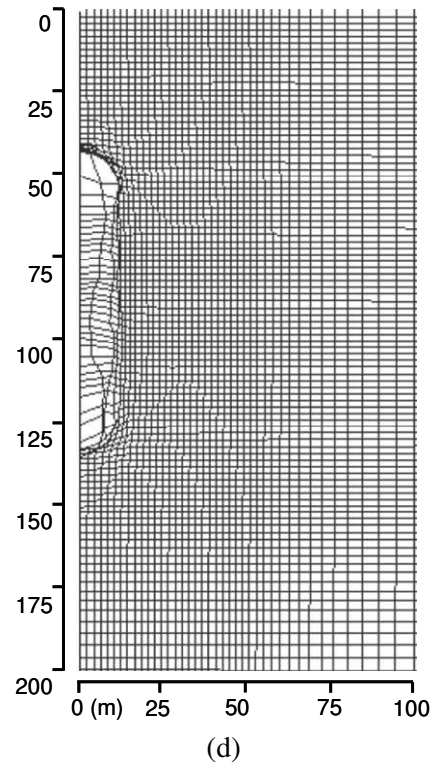


Figure S3. Deformation features of the formation for the case REF: (a) at initial, (b) after 1 yr, (c) after 2 yrs, (d) after 5 yrs, (e) after 10 yrs, and (f) after 20 yrs. Note that the displacements between the grid points in the images are amplified by the factor of 5.